Since January 2020 Elsevier has created a COVID-19 resource centre with free information in English and Mandarin on the novel coronavirus COVID-19. The COVID-19 resource centre is hosted on Elsevier Connect, the company's public news and information website.

Photodiagnosis and Photodynamic Therapy 40 (2022) 103157

Contents lists available at ScienceDirect

Photodiagnosis and Photodynamic Therapy

journal homepage: www.elsevier.com/locate/pdpdt

OCT and OCTA evaluation of vascular and morphological structures in the retina in recovered pediatric patients with COVID-19☆

Semra Tiryaki Demir [a,*], Nazan Dalgic [b], Sumeyra Keles Yesiltas [a], Emine Betul Akbas Ozyurek [a], Murat Karapapak [c], Saniye Uke Uzun [a], Dilek Guven [d]

[a] Department of Ophthalmology, Sisli Hamidiye Etfal Training and Research Hospital, University of Health Sciences, Istanbul, Turkey
[b] Department of Pediatric Infectious Diseases, Saryer Hamidiye Etfal Training and Research Hospital, University of Health Sciences, Istanbul, Turkey
[c] Department of Ophthalmology, Basaksehir City Hospital, University of Health Sciences, Istanbul, Turkey
[d] Department of Ophthalmology, Acibadem Maslak Hospital, Istanbul, Turkey

ARTICLE INFO

Keywords:
Peripapillary retinal nerve fiber layer
Choroidal thickness
Ganglion cell layer
Deep capillary plexus
Radial peripapillary capillary plexus
Optical coherence tomography

ABSTRACT

Background: Using OCT and OCTA imaging, we aimed to determine whether COVID-19 induces pathological changes in vascular and morphological structures in the pediatric retina.
Methods: The current prospective, cross-sectional, observational clinical study included recovered pediatric patients with COVID-19 evaluated between May 2020 and June 2020. Retinal vascular (radial peripapillary, superficial, and deep capillary plexus vessel densities) and morphological (peripapillary retinal nerve fiber, ganglion cell layer, retinal, and choroidal thickness) in the optic disk and macula regions were quantitively assessed using OCT and OCTA. Data were compared between COVID-19 patients and age-matched controls.
Results: The COVID-19 group included 32 eyes of 16 patients and the control group included 32 eyes of 16 cases. Fundus and biomicroscopic examinations revealed no signs of pathology in the COVID-19 group. Mean peripapillary retinal nerve fiber, ganglion cell layer, and choroidal thickness values were significantly greater in the COVID-19 group than in the control group ($p<0.05$). OCTA indicated that mean superficial and deep capillary plexus vessel densities, and choriocapillaris flow area values were significantly lower in the COVID-19 group than in the control group, whereas mean radial peripapillary capillary plexus vessel density values were significantly higher ($p<0.05$).
Conclusions: Even if fundus examination results appear normal in pediatric patients with COVID-19, vascular and morphological changes may be observed in the retina. Further studies with larger numbers of patients are needed to elucidate the clinical significance of vascular and morphological changes in this population.

1. Introduction

Having reached pandemic status in March 2020, novel coronavirus disease 2019 (COVID-19) continues to spread rapidly worldwide. Although COVID-19 occurs less frequently in pediatric patients than in adult patients, significant increases in the number of pediatric cases have been observed due to non-compliance with preventive measures (e.g., handwashing, face masks) [1].

For coronavirus to enter a potential host cell, appropriate receptors must be present. Human angiotensin converting enzyme-2 (ACE-2) is the functional host receptor for severe acute respiratory syndrome coronavirus 2 (SARS-CoV-2) [2]. Given that ACE-2 receptors are particularly abundant in the human retina, binding of SARS-CoV-2 may lead to various retinal pathologies [3]. The other host receptor is transmembrane protease serine 2 (TMPRSS2) [4].

Recent studies of eye involvement in pediatric patients with COVID-19 have included limited numbers of patients and have focused primarily on pathologies occurring in the anterior segment of the eye. To the best of our knowledge, there are few studies investigating posterior segment involvement in this age group [5–10].

Optical coherence tomography (OCT) and OCT angiography (OCTA) are frequently used for detailed, non-invasive evaluation of the posterior segment of the eye. OCT can be used to quantitatively assess retinal, choroidal, retinal nerve fiber, and ganglion cell layer thickness, while

☆ This manuscript was presented as an oral presentation at the EURETINA 2021 Virtual Congress.

* Corresponding author.
E-mail address: dr-semra@hotmail.com (S. Tiryaki Demir).

https://doi.org/10.1016/j.pdpdt.2022.103157
Received 30 August 2022; Received in revised form 8 October 2022; Accepted 11 October 2022
Available online 14 October 2022

OCTA can be used to assess the densities of different vascular plexuses in the macula and optic disk[11,12].

Using OCT and OCTA, the present study aimed to determine whether COVID-19 can induce pathology in the posterior segment of the eye in pediatric patients. We also compared quantitative OCT and OCTA data between pediatric patients with COVID-19 and healthy controls.

2. Patients and methods

2.1. Study participants

This study was approved by the local human research ethics committee, in accordance with the Declaration of Helsinki, and written informed consent was obtained from all participants' parents or guardians (2829/2020).

In the current prospective, cross-sectional, observational clinical study, we analyzed data from pediatric patients with COVID-19 who had been evaluated between May 2020 and June 2020. COVID-19 test results were positive in all patients. All patients underwent treatment at the Pediatric Infection Clinic of our hospital between March 2020 and May 2020. The healthy controls consisted of subjects who had visited the ophthalmology clinic for routine ocular examinations. Because right and left eye measurements tended to differ within the same subject, both eyes of all subjects were analyzed in the study.

Complete ophthalmologic examinations were performed for all participants by the two retina specialist (S.T.D and D.G). Examinations performed on subjects included the best corrected visual acuity (BCVA) according to the Snellen chart, intraocular pressure, and anterior and posterior segment examinations. Spectral-domain OCT (AngioVue, Optovue, Fremont, CA) was used to evaluate thickness in various retinal, choroidal, and peripapillary retinal nerve fiber structures. A different spectral-domain OCT device (3DOCT-2000; Topcon Inc., Tokyo, Japan) was used to analyze fundus autofluorescence (FAF), macular retinal nerve fiber thickness, and ganglion cell layer thickness. In addition, OCTA (AngioVue, Optovue, Fremont, CA) was used to evaluate different vascular plexuses in the macula and optic disk. OCT and OCTA imaging was performed after pupil dilatation (using cyclopentolate HCL 1% eye drops). To exclude diurnal variations, all examinations were performed at the same time of day (10 a.m.- 1 p.m.)

Inclusion criteria for the patient group were as follows: (a) age 6–18 years; (b) positive 2019-nCoV real-time polymerase chain reaction (PCR) test from a sample obtained by swabbing the nasal or oral region, or positive results for immunoglobulin M (IgM) and IgG antibodies for COVID-19 as determined via enzyme-linked immunosorbent assay (ELISA); (c) maintenance of treatment for COVID-19 at home (i.e., outpatient treatment) or completion of treatment; (d) a period of at least 15 days from the onset of symptoms (fever, cough, shortness of breath, myalgia, headache, nausea, vomiting, diarrhea, loss of smell and taste, etc.) to reduce the risk of transmitting the disease; (e) and the ability to fixate on a light target and maintain a stable head position during image capture. The controls consisted of healthy children with best corrected visual acuity (BCVA) of 20/20 using the Snellen chart who did not have any ocular or systemic disorders, and had spherical and cylindrical refractive errors $\leq$ 3.00 diopter.

Patients continuing to exhibit poor general condition and those hospitalized due to COVID-19 or other systemic diseases were excluded. Additional exclusion criteria were as follows: (a) a period of less than 15 days from the onset of symptoms due to the risk of transmission of the disease; (b) negative COVID-19 test results; (c) corneal opacity or cataract affecting the media and preventing detailed imaging; (d) high refractive errors (including myopia, hyperopia, and astigmatism of >3.0 diopter); (e) previous ocular surgery, laser treatments, or trauma; (f) the presence of ocular or neurologic disease, smoking; (g) inability to cooperate during the examination; (h) and poor imaging quality during the relevant examinations (signal strength index < 6/10).

2.2. Optical coherence tomography measurements

1. *Retinal thickness measurements*

The foveal center was defined as the location at which the foveal pit is deepest. The measurements were made in the following areas; a 1×1 mm circle as the fovea, and a 3×3 mm annulus other than the fovea as the parafovea. The parafoveal area was examined as nasal, superior, temporal, and inferior quadrants. The values of central foveal thickness (CFT) and retinal thickness (RT) of the four parafoveal quadrants were measured automatically. The CFT was measured as the distance from the deepest point of the foveal pit to the inner border of the retinal pigment epithelium (RPE).

2. *Choroidal thickness measurements*

Choroidal thickness (CT) was defined as the distance between the base of the RPE and choroidoscleral boundary. Each measurement was performed at the subfoveal and 0.75 mm, and 1.5 mm nasal (N1CT, N2CT) and temporal (T1CT, T2CT), respectively, to fovea using the manual calipers provided with the software of the device (Fig. 1a).

3. *Peripapillary retinal nerve fiber layer thickness measurements*

A circle with 3.4 mm in diameter centered on the papilla was automatically placed, and a 1.0-mm wide round annulus extending from the optical disk boundary was considered the peripapillary region. The mean thicknesses of total peripapillary retinal nerve fiber layer thickness (pRNFLT) and four peripapillary quadrants were determined with automatic segmentation (Fig. 1b).

4. *Ganglion cell layer thickness measurements*

A 7×7-mm macular scan protocol was used. These scans were automatic segmented into the ganglion cell layer with the inner plexiform layer (GCL+IPL), and ganglion cell complex (GCC) (composed of the macular retinal nerve fiber layer + GCL+IPL) (Fig. 1c).

2.3. Optical coherence tomography angiography measurements

The OCTA examination was performed using the standard macular and peripapillary protocol. All of the eye scans were of a 3×3 mm scanning area centered on the fovea and a 4.5×4.5 mm scanning area centered on the papilla. All of the OCT-A images reviewed to ensure the correct segmentation and identify poor-quality scans with motion artifacts or blurred images, or where the data were insufficient for proper analysis. The device included the projection artefact removal algorithm [13].

1. *Foveal avascular zone area*

The foveal avascular zone (FAZ) is the retinal capillary free area located in the central fovea. The FAZ area (mm^2) was determined from the en face OCTA images. The FAZ diameter was automatically calculated by the non-flow mode in each image of the auto-segmented retina (Fig. 1d).

2. *Superficial capillary plexuses and deep capillary plexus vessel densities*

The automated segmentation of the superficial capillary plexuses (SCP, slab from ILM to inner plexiform layer), deep capillary plexuses (DCP, slab from inner plexiform layer to outer plexiform layer) were obtained using the manufacturer's built-in software. The vessel densities (%) (VD) of SCP and DCP in foveal and four parafoveal quadrants were automatically measured (Fig. 1e, f).

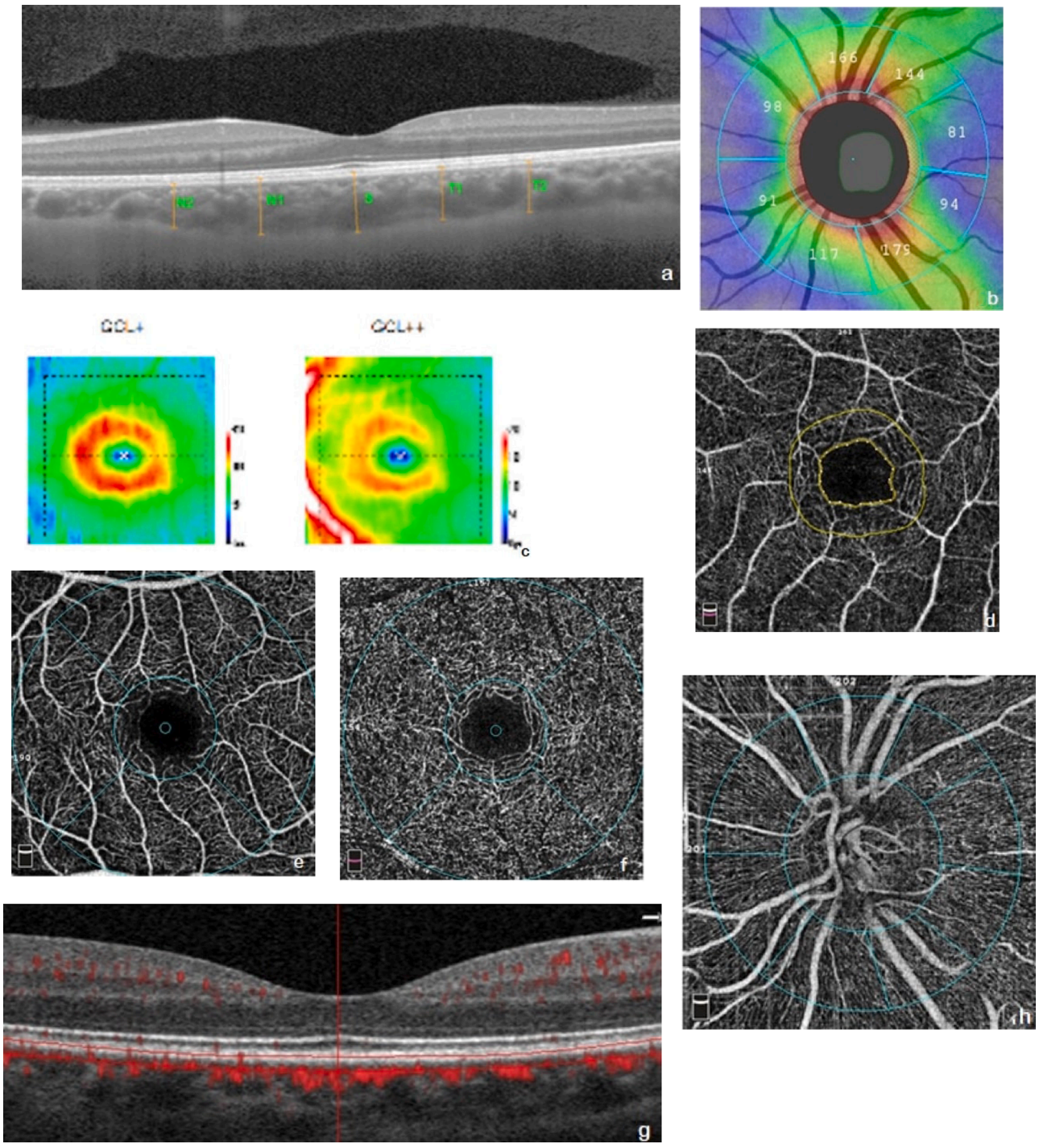

Fig. 1. Optical coherence tomography and optical coherence tomography angiography imaging examples of some pediatric patients with novel coronavirus disease 2019. **1a**: Choroidal thickness measurements. **1b**: Peripapillary retinal nerve fiber layer thickness measurements. **1c**: Ganglion cell layer thickness measurements. **1d**: Foveal avascular zone area measurement. **1e**: Superficial capillary plexuses vessel densities measurements **1f**: Deep capillary plexus vessel densities measurement. **1 g**: Flow area in the choriocapillaris layer measurement. **1h**: Radial peripapillary capillary plexus vessel densities measurements.

3. *Flow area in the choriocapillaris layer*

The automated segmentation of the choriocapillaris (CC; slab 29–49 μm under the RPE) were obtained using the manufacturer's built-in software. The flow area (in mm^2) of the CC layer was also measured automatically by flow mode (Fig. 1g).

4. *Radial peripapillary capillary plexus vessel densities*

The VD of peripapillary areas were examined. The radial peripapillary capillary plexus (RPCP) slab was obtained from the top of ILM to 70.2 μm below it. Peripapillary VD was defined as the percentage of the area occupied by the vessels in the peripapillary region. The VD of whole peripapillary, and upper half and lower half peripapillary areas were automatically measured (Fig. 1h).

2.4. Statistical analysis

Mean, standard deviation, and ratios were calculated and used in statistical analysis. Data distributions were assessed using the Kolmogorov-Smirnov test. Analysis of variance and the post-hoc Tukey test and the Mann-Whitney U test were used for the analysis of quantitative independent data, depending on the distributions of the variables being compared. The chi-square test was used to analyze independent data. SPSS 22.0 software was used to conduct statistical analyses. $p < 0.05$ was deemed to indicate statistical significance.

3. Results

The present study included 64 eyes in 32 patients: 32 eyes of 16 patients in the COVID-19 group and 32 eyes of 16 patients in the control group. Each group included 12 girls and 4 boys. Examinations were performed a mean of 34.8±9.8 (range: 18–54) days after the onset of COVID-19 symptoms. The mean age was 13.1±3.7 years in the COVID-19 group and 13.2±3.3 years in the control group (p=0.978). Demographic data, laboratory test results, lung imaging findings, and management data of the patients are shown in Table 1. BCVA (20/20) and pupillary reflexes were normal in all eyes. The mean intraocular pressure was 16.8±2.8 mmHg in the COVID-19 group and 15.5±2.5 mmHg in the control group (p=0.152). Biomicroscopic and fundus examinations revealed no signs of pathology in the COVID-19 group. FAF findings were also normal in the COVID-19 group.

Mean values for RT, CT, pRNFLT, and GCL thickness in both groups are shown in Table 2. All mean CT measurements were greater in the COVID-19 group than in the control group. However, while this difference was significant for mean nasal and temporal CT (p<0.05), the groups exhibited no significant difference in mean subfoveal CT (p=0.283). All mean pRNFLT measurements were greater in the COVID-19 group than in the control group. Mean values in the full peripapillary region (p=0.002), nasal quadrant (p=0.026), and superior quadrant (p<0.001) significantly differed between the groups. All mean GCL+IPL and GCC thickness values were greater in the COVID-19 group than in the control group (p<0.05). There were no significant differences in mean RT between the groups (p>0.05).

Mean FAZ diameter, SCP-VD, DCP-VD, choriocapillaris flow area, and RPCP-VD measurements for both groups are shown in Table 3. Although all mean SCP-VD and DCP-VD values were lower in the COVID-19 group than in the control group, all mean RPCP-VD values were higher. All mean parafoveal DCP-VD, parafoveal inferior SCP-VD, and choriocapillaris flow area values were significantly lower in the COVID-19 group than in the control group (p<0.05). Mean whole peripapillary, upper half, and lower half RPCP-VD values were significantly higher in the COVID-19 group than in the control group (p<0.05). There

Table 2
Mean optical coherence tomography values for the macular and optic disk regions in pediatric patients with novel coronavirus disease 2019 (COVID-19) and healthy controls.

OCT variables	COVID-19 Group(n = 32 eyes)Mean ± SD or n (50%)	Control Group(n =32 eyes)Mean ± SD or n (50%)	p
Retinal Thickness (μ)			
CFT	239.1 ± 21.8	241.2 ± 15.8	0.893 M
Parafoveal temporal	303.7 ± 16.3	299.1 ± 10.5	0.177 t
RT	317.9 ± 14.8	314.5 ±11.4	0.308 t
Parafoveal superior	315.9 ± 16.9	316.3 ± 11.7	0.925 t
RT	314.1 ± 14.9	311.5 ± 10.5	0.425 t
Parafoveal nasal RT			
Parafoveal inferior			
RT	315.5 ± 67	299.4 ± 50.8	0.283 t
	311.8 ± 60.1	275.6 ± 47.2	**0.010 t**
Choroidal	287.4 ± 61.8	251.8 ± 53.5	**0.017 t**
thickness (μ)	319.1 ± 59	290.3 ± 47.4	**0.035 t**
Subfoveal CT	317.8 ± 51.7	281.5 ± 51.4	**0.007 t**
N1CT			
N2CT			
T1CT	117.8 ± 12.3	109.4 ± 7.6	**0.002 t**
T2CT	77.4 ± 11.6	75.9 ± 8.7	0.553 t
	150.6 ± 20.6	141.4 ± 10.1	0.078 M
p RNFLT (μ)	103.1 ± 18.2	94 ± 14.7	**0.026 M**
Whole peripapillary	144.3 ± 13.3	128.2 ± 12	**<0.001**
Temporal quadrant			**t**
Inferior quadrant			
Nasal quadrant	73 ± 4.7	69.7 ± 3.5	
Superior quadrant	74.5 ± 6.5	69.4 ± 3.1	**0.002 t**
	73.5 ± 5.1	69.6 ± 3	**0.002 t**
Ganglion Cell	106 ± 6.3	102.8 ± 5.1	**0.008 t**
Layers Thicknesses	107.8 ± 8.4	103.7 ± 4.7	**0.031 t**
(μ)	106.7 ± 7.1	103.2 ± 4.3	**0.020 M**
GCL+IPL superior half			**0.020 M**
GCL+IPL inferior half			
GCL+IPL total			
GCC superior half			
GCC inferior half			
GCC total			

M: Mann-Whitney U test, t: t test
OCT: optical coherence tomography, CFT: central foveal thickness, RT: retinal thickness, CT: choroidal thickness, N1CT: choroidal thickness 0.75 mm nasal to the fovea, N2CT: choroidal thickness 1.5 mm nasal to the fovea, T1CT: choroidal thickness 0.75 mm temporal to the fovea, T2CT: choroidal thickness 1.5 mm temporal to the fovea, pRNFLT: peripapillary retinal nerve fiber layer thickness, GCL+IPL: ganglion cell layer with the inner plexiform layer, GCC: ganglion cell complex.

Table 1
Demographic data, laboratory tests, lung imaging findings, and management of the pediatric COVID-19 patients.

Parameters examined	C1	C2	C3	C4	C5	C6	C7	C8	C9	C10	C11	C12	C13	C14	C15	C16
Age (y)	14	13	16	17	11	16	15	17	17	16	6	9	17	9	9	9
Sex (female, male)	F	F	F	F	F	M	F	F	F	M	M	F	F	M	F	F
Ocular examination time (d)	37	31	35	32	30	43	37	54	22	18	37	35	47	44	38	18
WBC	12.7	9.28	5.67	4.2	7.7	6.6	5.92	7.58	3.58	9.59	3.05	10.46	5.35	14.2	5.56	6.55
Lymphocytes	0.83	3.95	1.44	42.20	1.91	2.95	0.93	2.06	1.67	1.63	1.41	1.2	0.8	2.9	0.89	1.0
Neutrophil	11.38	4.84	3.96	2.21	5.16	2.85	4.32	4.56	1.64	7.58	1.19	8.35	3.58	9.98	4.06	5.31
CRP	6.29	0.44	1.33	10.76	1.05	6.39	1.92	32.7	5.5	0.81	7.27	1.05	2.28	13.2	1.88	95.27
Ferritin	13.1	19.4	18.6	75.2	16.6	79.9	30.2	28	95.4	58.1	28.8	34.8	13.3	28.5	35.9	256
D-dimer	308	273	1270	2370	543	908	402	873	361	471	NA	140	565	415	NA	2340
CK	52	83	N/A	46	115	199	85	122	51	110	115	NA	NA	81	90	NA
CK-MB	N/A	1.8	1.5	0.2	1.5	N/A	1.7	NA	0.3	2.2	NA	2.3	1.6	NA	NA	2.7
Lung CT (inflammatory lesions)	+	-	-	+	-	+	-	+	+	+	-	-	-	-	-	+
Oral or i.v antibiotic therapy	+	-	-	+	-	+	-	+	+	+	-	-	-	-	-	+
Vitritis detected by OCT	+	+	+	+	+	-	-	-	-	-	-	-	-	-	-	-

C: case, y: years, d: days, WBC: leukocytes, CRP: C-reactive protein CRP, CK: Creatine kinase, CK-MB: Creatine kinase MB isoenzyme, CT: computerized tomography, OCT: optical coherence tomography, NA: not available.

Table 3
Mean optical coherence tomography angiography values for the macular and peripapillary regions in pediatric patients with novel coronavirus disease 2019 (COVID-19) and healthy controls.

OCTA variables	COVID-19 Group (n = 32 eyes)Mean ±SD or n (50%)	Control Group(n = 32 eyes)Mean ±SD or n (50%)	*p*
Macula OCTA (%)			
FAZ (mm^2)	0.307 ± 0.11	0.288 ± 0.10	0.477 t
Foveal SCP-VD	16.7 ± 6.6	18 ± 5.8	0.413 t
Parafoveal SCP-VD	48.3 ± 5.1	50.5 ± 2.6	0.175 M
Parafoveal temporal	47.1 ± 5.4	49.1 ± 2.5	0.274 M
SCP-VD	49.8 ± 4.8	51.4 ± 3.4	0.139 t
Parafoveal superior	47.4 ± 5.4	49.5 ± 2.4	0.219 M
SCP-VD	48.7 ± 5.6	51.7 ± 3.3	**0.049 M**
Parafoveal nasal	32.1 ± 7.8	34.1 ± 7.7	0.310 t
SCP-VD	53.1 ± 2.8	55.2 ± 3.5	**0.014 t**
Parafoveal inferior	53.9 ± 2.8	55.7 ± 2.8	**0.013 t**
SCP-VD	52.7 ± 2.9	55.1 ± 4.3	**0.010 t**
Foveal DCP-VD	53.1 ± 3.1	56 ± 3.5	**0.001 t**
Parafoveal DCP-VD	52.8 ± 3.7	54.3 ± 4.3	0.133 t
Parafoveal temporal DCP-VD	2.069 ± 0.15	2.229 ± 0.78	**<0.001 M**
Parafoveal superior DCP-VD	52.8 ± 2.9	50.8 ± 2.4	
Parafoveal nasal DCP-VD	52.8 ± 3.1	50.7 ± 2.4	**0.004 t**
Parafoveal inferior DCP-VD	53 ± 3	50.9 ± 2.7	**0.005 t**
Choriocapillaris flow area (mm^2)			**0.007 t**
Peripapillary OCTA VD (%)			
Whole peripapillary			
Upper half peripapillary			
Lower half peripapillary			

M: Mann-Whitney U test, t: t test
OCTA: optical coherence tomography angiography, FAZ: foveal avascular zone diameter, SCP-VD: vessel densities of superficial capillary plexuses, DCP-VD: vessel densities of deep capillary plexuses, VD: vessel density.

were no significant differences in mean FAZ diameter (p=0.477) between the groups. Cotton wool spots, retinal hemorrhages, retinitis-like findings and focal or multifocal capillary drop-out areas were not detected on OCT and OCTA images in any patient.

4. Discussion

In the present study, we aimed to investigate the effects of COVID-19 on posterior segment structures in the eye in pediatric patients with COVID-19. Biomicroscopic and fundus examinations revealed no signs of pathology. OCT indicated that mean CT, pRNFLT, GCL+IPL thickness, and GCC thickness values were higher in the COVID-19 group than in the control group. In contrast, OCTA revealed that mean SCP-VD, DCP-VD, and choriocapillaris flow area values were lower in the COVID-19 group than in the control group, while mean RPCP-VD values were higher.

Children play an important role in the spread of COVID-19 [1]. However, symptoms of the disease tend to be less frequent and less severe in children than in adults [14]. Differences in the clinical features and laboratory characteristics of COVID-19 are thought to be due to differences in the maturity and functional status of ACE-2 between children and adults [1]. ACE-2 is an important component of the renin–angiotensin system (RAS), which plays an essential role in maintaining homeostasis in humans. ACE-2 antagonizes the activation of the classical RAS system and protects against organ damage [15]. ACE-2 receptors are widely expressed in many parts of the body, including the heart, blood vessels (vascular endothelial and smooth cells), intestines, lungs, kidneys, testes, and brain [16]. Research has indicated that ACE-2 is also present in the human retina, aqueous humor and choroid [3,17,18]. ACE-2 receptors mediate the entry of SARS-CoV-2 into the cell [19]. Down-regulation of ACE-2 caused by SARS-CoV-2 entry can lead to hyper-coagulation, progression of inflammation, and enhanced thrombosis [16].

More recently, few manuscripts have been reported evaluating retinal and choroidal thickness changes in pediatric patients with COVID-19 by OCT imaging and comparing them with healthy children [6,8,9]. Zengin et al. [6] reported that the foveal thickness was thinner and the CT was thicker in children with COVID-19 compared to healthy children. Burgos-Blasco et al. [9] showed that there was no significant difference in RT between the two groups. Akpolat et al. [8] reported that the CT was thinner in children with COVID-19 than in healthy children. We observed that while CT values were significantly greater in pediatric patients with COVID-19 than controls, there was no difference in RT. The increase in CT may have been caused by intraocular inflammation resulting from SARS-CoV-2 infection.

Recent studies have reported that SARS-CoV-2 may also exhibit neuroinvasion and neuroinflammation [20–25]. The inner retina is a neuronal tissue and can be damaged by SARS-CoV-2 [26]. Retinal nerve fiber and ganglion cell layer thickness changes were evaluated in pediatric patients with COVID-19 by OCT imaging and comparing them with healthy children [8,9]. Burgos-Blasco et al. [9] reported that the pRNFLT and macular GCL thickness was thicker in patients with COVID-19 compared to healthy subjects. Akpolat et al. [8] reported that the pRNFLT was thicker in patients with COVID-19 compared to healthy subjects, while the GCL was thinner. In the present study, OCT revealed that pRNFLT, GCL+IPL thickness, and GCC thickness values were significantly greater in the COVID-19 group than in the control group. These findings suggest that patients with COVID-19 exhibited thickening of the GCL and NFLs consisting of ganglion cell axons. Such thickening may result from the infiltration of immune cells and release of proinflammatory mediators in the early stage of the disease. Furthermore, this finding may indirectly indicate that SARS-CoV-2 is a neurotropic virus.

It has been reported that COVID-19 can cause microvascular damage due to hypercoagulability or diffuse endothelial inflammation [27–30]. OCTA, a non-invasive imaging modality, can show images of blood flow in all the vascular layers of the retina [31]. Vascular structures around the macula and optic disk in pediatric patients recovering from COVID-19 were evaluated with OCTA and compared with healthy children [5–7,10]. Guemes-Villahoz et al. [5] reported that SCP-VD, macular perfusion density, and peripapillary fluw index were significantly increased in patients compared to controls. Zengin et al. [6] reported that macular vessel density and perfusion density were lower and the FAZ area was larger in patients compared to controls. Our OCTA findings demonstrated that choriocapillaris flow area, SCP-VD, and DCP-VD (i.e., blood supply to the macular region) were significantly decreased in pediatric patients with COVID-19, relative to values observed in controls. Such findings may be explained by hyper-coagulation and enhanced thrombosis due to COVID-19. However, surprisingly, RPC-VD values (i.e., blood supply to the optic disk region) were significantly higher in the COVID-19 group than in the control group. Photoreceptors and ganglion cells located in the macular region require high levels of oxygen. An increase in RPC-VD may represent an attempt to compensate for COVID-19-induced ischemia in the macular region.

The current study had many strengths. To our knowledge, our study is the first to evaluate in detail both vascular and morphological structures of the macula and peripapillary region in pediatric patients with COVID-19 using OCT and OCTA. OCT revealed an increase in GCL, NFL, and CL thickness in the COVID-19 group. In addition, OCTA revealed that VD decreased for capillary plexuses providing blood supply to the macular region and increased for those providing blood supply to the optic disk region. None of our patients in present study had a history of chronic illness, smoking, or drug use that could affect these OCT and

OCTA data. Nonetheless, our study had its limitations, including its small sample size. In addition, detailed examinations were performed for the posterior pole only, and we were unable to evaluate the peripheral retina via wide-field retinal imaging. Due to its invasive nature, we were also unable to perform fluorescein angiography. We did not evaluate the severity of COVID-19 symptoms or the correlation of virus titer with the degree of morphological and vascular changes in this study.

In conclusion, our findings demonstrate that OCT and OCTA are useful for the non-invasive evaluation of morphological and vascular characteristics of the macula and optic disk in pediatric patients with COVID-19. Even if fundus examination results appear normal in these patients, morphological and vascular differences may exist. However, the long-term pathological effects of these morphological and vascular changes remain to be determined. Further studies including larger sample sizes are required to elucidate the clinical significance of structural and vascular changes in pediatric patients with COVID-19.

CRediT authorship contribution statement

Semra Tiryaki Demir: Writing – original draft, Supervision, Project administration, Methodology, Data curation, Conceptualization. **Nazan Dalgic:** . **Sumeyra Keles Yesiltas:** . **Emine Betul Akbas Ozyurek:** . **Murat Karapapak:** . **Saniye Uke Uzun:** . **Dilek Guven:** .

Declaration of Competing Interest

Semra Tiryaki Demir declares that she has no conflict of interest. Nazan Dalgic declares that she has no conflict of interest. Sumeyra Keles Yesiltas declares that she has no conflict of interest. Emine Betul Akbas Ozyurek declares that she has no conflict of interest. Murat Karapapak declares that he has no conflict of interest. Saniye Uke Uzun declares that she has no conflict of interest. Dilek Guven declares that she has no conflict of interest.

Funding

This research did not receive any specific grant from funding agencies in the public, commercial, or not-for-profit sectors.

Ethical approval

All procedures performed in studies involving human participants were in accordance with the ethical standards of the institutional and/or national research committee and with the 1964 Helsinki declaration and its later amendments or comparable ethical standards.

Informed consent

Informed consent was obtained from parents of all participants included in the study.

References

[1] X Cui, T Zhang, J Zheng, J Zhang, P Si, Y Xu, et al., Children with Coronavirus Disease 2019 (COVID-19): a review of demographic, clinical, laboratory and imaging features in pediatric patients, J. Med. Virol. 92 (2020) 1501–1510, https://doi.org/10.1002/jmv.26398.

[2] AR Bourgonje, AE Abdulle, W Timens, JL Hillebrands, GJ Navis, SJ Gordijn, et al., Angiotensin-converting enzyme-2 (ACE2), SARS-CoV-2 and pathophysiology of coronavirus disease 2019 (COVID-19), J. Pathol. 251 (2020) 228–248, https://doi.org/10.1002/path.5471.

[3] P Senanayake, J Drazba, K Shadrach, A Milsted, E Rungger-Brandle, K Nishiyama, et al., Angiotensin II and its receptor subtypes in the human retina, Invest. Ophthalmol. Vis. Sci. 48 (2007) 3301–3311, https://doi.org/10.1167/iovs.06-1024.

[4] M Hoffmann, H Kleine-Weber, S Schroeder, N Krüger, T Herrler, S Erichsen, et al., SARS-CoV-2 cell entry depends on ACE2 and TMPRSS2 and is blocked by a clinically proven protease inhibitor, Cell. 181 (2020) 271–280, https://doi.org/10.1016/j.cell.2020.02.052.

[5] N Guemes-Villahoz, B Burgos-Blasco, P Perez-Garcia, JI Fernández-Vigo, L Morales-Fernandez, J Donate-Lopez, et al., Retinal and peripapillary vessel density increase in recovered COVID-19 children by optical coherence tomography angiography, J. AAPOS 25 (6) (2021), https://doi.org/10.1016/j.jaapos.2021.06.004, 325.e1-325.e6.

[6] N Zengin, YZ. Güven, Retinal microvascular and perfusional disruption in paediatric COVID-19: a case control optical coherence tomography angiography study, Photodiagnosis Photodyn. Ther. 36 (2021 Dec), 102577, https://doi.org/10.1016/j.pdpdt.2021.102577.

[7] T Cetinkaya, MM Kurt, H Cetinkaya, C. Akpolat, Analysis of Microvasculature in Children Recovered from COVID-19 Using Swept-Source OCT/OCTA Technology, Ocul. Immunol. Inflamm. (2022) 1–7, https://doi.org/10.1080/09273948.2022.2054431. Apr 11.

[8] C Akpolat, T Cetinkaya, MM. Kurt, A pediatric COVID-19 study: retinal nerve fiber layer, ganglion cell layer, and alterations in choroidal thickness in swept-source OCT measurements, Klin. Monbl. Augenheilkd. 239 (7) (2022 Jul) 916–922, https://doi.org/10.1055/a-1785-3863.

[9] B Burgos-Blasco, N Güemes-Villahoz, L Morales-Fernandez, I Callejas-Caballero, P Perez-Garcia, J Donate-Lopez, et al., Retinal nerve fibre layer and ganglion cell layer changes in children who recovered from COVID-19: a cohort study, Arch. Dis. Child. 107 (2) (2022) 175–179, https://doi.org/10.1136/archdischild-2021-321803.

[10] OB Comba, M Karakaya, S Albayrak, E. Yalçın, Early-term optical coherence tomography angiographic findings in pediatric patients infected with COVID-19, Ocul. Immunol. Inflamm. (2022) 1–5, https://doi.org/10.1080/09273948.2022.2027470. Jan 26.

[11] KA Maccora, S Sheth, JB. Ruddle, Optical coherence tomography in paediatric clinical practice, Clin. Exp. Optom. 102 (2019) 300–308, https://doi.org/10.1111/cxo.12909.

[12] T Li, Y Jia, S Wang, A Wang, L Gao, C Yang, et al., Retinal microvascular abnormalities in children with type 1 diabetes mellitus without visual impairment or diabetic retinopathy, Invest. Ophthalmol. Vis. Sci. 60 (2019) 990–998, https://doi.org/10.1167/iovs.18-25499.

[13] ST Garrity, NA Iafe, N Phasukkijwatana, X Chen, D Sarraf, Quantitative analysis of three distinct retinal capillary plexuses in healthy eyes using optical coherence tomography angiography, Invest. Ophthalmol. Vis. Sci. 58 (2017) 5548–5555, https://doi.org/10.1167/iovs.17-22036.

[14] Y Dong, X Mo, Y Hu, X Qi, F Jiang, Z Jiang, et al., Epidemiology of COVID-19 among children in China, Pediatrics 145 (6) (2020 Jun), e20200702, https://doi.org/10.1542/peds.2020-0702.

[15] H Cheng, Y Wang, GQ. Wang, Organ-protective effect of angiotensin-converting enzyme 2 and its effect on the prognosis of COVID-19, J. Med. Virol. 92 (2020) 726–730, https://doi.org/10.1002/jmv.25785.

[16] P Verdecchia, C Cavallini, A Spanevello, F. Angeli, The pivotal link between ACE2 deficiency and SARS-CoV-2 infection, Eur. J. Intern. Med. 76 (2020) 14–20, https://doi.org/10.1016/j.ejim.2020.04.037.

[17] M Holappa, J Valjakka, A. Vaajanen, Angiotensin (1-7) and ACE2, "The Hot Spots" of renin-angiotensin system, detected in the human aqueous humor, Open Ophthalmol. J. 9 (2015) 28–32, https://doi.org/10.2174/1874364101509010028.

[18] L Chen, M Liu, Z Zhang, K Qiao, T Huang, M Chen, et al., Ocular manifestations of a hospitalised patient with confirmed 2019 novel coronavirus disease, Br. J. Ophthalmol. 104 (2020) 748–751, https://doi.org/10.1136/bjophthalmol-2020-316304.

[19] AC Walls, YJ Park, MA Tortorici, A Wall, AT McGuire, D. Veesler, Structure, function, and antigenicity of the SARS-CoV-2 spike glycoprotein, Cell 181 (2020) 281–292, https://doi.org/10.1016/j.cell.2020.02.058.

[20] L Mao, H Jin, M Wang, Y Hu, S Chen, Q He, et al., Neurologic manifestations of hospitalized patients with coronavirus disease 2019 in Wuhan, China, JAMA Neurol. 77 (2020) 683–690, https://doi.org/10.1001/jamaneurol.2020.1127.

[21] A Varatharaj, N Thomas, MA Ellul, NWS Davies, TA Pollak, EL Tenorio, et al., Neurological and neuropsychiatric complications of COVID-19 in 153 patients: a UK-wide surveillance study, Lancet Psychiatry 7 (2020) 875–882, https://doi.org/10.1016/S2215-0366(20)30287-X.

[22] RW Paterson, RL Brown, L Benjamin, R Nortley, S Wiethoff, T Bharucha, et al., The emerging spectrumof COVID-19 neurology: clinical, radiological and laboratory findings, Brain 143 (2020) 3104–3120, https://doi.org/10.1093/brain/awaa240.

[23] G Tsivgoulis, L Palaiodimou, AH Katsanos, V Caso, M Köhrmann, C Molina, et al., Neurological manifestations and implications of COVID-19 pandemic, Ther. Adv. Neurol. Disord. 13 (2020), 1756286420932036, https://doi.org/10.1177/1756286420932036.

[24] A Achar, C Ghosh, COVID-19-Associated Neurological Disorders: The Potential Route of CNS Invasion and Blood-Brain Relevance, Cells 9 (2020) 2360, https://doi.org/10.3390/cells9112360.

[25] BN Harapan, HJ. Yoo, Neurological symptoms, manifestations, and complications associated with severe acute respiratory syndrome coronavirus 2 (SARS-CoV-2) and coronavirus disease 19 (COVID-19), J. Neurol. 268 (9) (2021 Sep) 3059–3071, https://doi.org/10.1007/s00415-021-10406-y.

[26] A Pryce-Roberts, M Talaei, NP Robertson, Neurological complications of COVID-19: a preliminary review, J. Neurol. 267 (2020) 1870–1873, https://doi.org/10.1007/s00415-020-09941-x.

[27] JM Connors, JH. Levy, COVID-19 and its implications for thrombosis and anticoagulation, Blood 135 (2020) 2033–2040, https://doi.org/10.1182/blood.2020006000.

[28] H Fogarty, L Townsend, C Ni Cheallaigh, C Bergin, I Martin-Loeches, P Browne, et al., More on COVID-19 coagulopathy in Caucasian patients, Br. J. Haematol. 189 (2020) 1060–1061, https://doi.org/10.1111/bjh.16791.
[29] N Tang, D Li, X Wang, Z Sun, Abnormal coagulation parameters are associated with poor prognosis in patients with novel coronavirus pneumonia, J. Thromb. Haemost. 18 (2020) 844–847, https://doi.org/10.1111/jth.14768.
[30] Z Varga, AJ Flammer, P Steiger, M Haberecker, R Andermatt, AS Zinkernagel, et al., Endothelial cell infection and endotheliitis in COVID-19, Lancet 395 (10234) (2020) 1417–1418, https://doi.org/10.1016/S0140-6736(20)30937-5.
[31] RF Spaide, JG Fujimoto, NK Waheed, SR Sadda, G. Staurenghi, Optical coherence tomography angiography, Prog. Retin. Eye Res. 64 (2018) 1–55, https://doi.org/10.1016/j.preteyeres.2017.11.003.